FITLABGUI - A VERSATILE TOOL FOR DATA ANALYSIS, SYSTEM IDENTIFICATION AND HELICOPTER HANDLING QUALITIES ANALYSIS

Susanne Seher-Weiss
DLR (German Aerospace Center), Institute of Flight Systems
Lilienthalplatz 7, 38108 Braunschweig, Germany
susanne.seher-weiss@dlr.de

ABSTRACT

Traditionally, the DLR Institute of Flight Systems operates both fixed- and rotary-wing flying test vehicles. The research topics associated with these vehicles include time and frequency domain data analysis, simulation model development for flight control law design, and handling qualities evaluation. Over the years, the MATLAB-based software FitlabGui was developed that allows to perform these tasks with a single tool. The paper describes the functionality of FitlabGui and illustrates the software with application examples from different research projects conducted at DLR.

NOMENCLATURE

Symbols

A, B, C, D	state space representation of dyn. system
b_x, b_y	bias parameters of the state resp. observation equations
F	transfer function
f	frequency, Hz
f_1	fundamental frequency
f_c	Nyquist frequency
G_{uu}, G_{yy}	input and output autospectra
G_{uy}	cross spectrum
H	frequency response
J	cost function
L	leakage term
N	number of data points
N_ω	number of frequency points
R	covariance matrix of measurement noise
S	spectral density matrix of meas. noise
s	Laplace variable
T	length of time interval, s
t	time, s
u	control input vector
U, V, X, Y, Z	Fourier transforms of u, v, x, y, z
v	measurement noise vector
W	weighting function/matrix
x	state vector
y	observation vector
z	measurement vector
Δt	sampling interval, s
ϵ_r	random error
ζ	damping ratio
γ^2_{uy}	coherence between u and y
$\sigma(\ldots)$	standard deviation
τ	time delay, s
ω	frequency, rad/s
ω_n	natural frequency
$\angle$	phase angle, deg
$\lvert\ldots\rvert$	amplitude

Superscripts

$*$	conjugate transpose of complex matrix
$\hat{}$	optimal value

Abbreviations

ACT/FHS	Active Control Technology/Flying Helicopter Simulator
FR	frequency response
FT	Fourier transform
HQ	handling qualities
LPM	local polynomial method
LTI	linear time-invariant
MISO	multi input / single output
ML	maximum likelihood
MTE	mission task element
TAT	target acquisition and tracking
TF	transfer function
ZPK	zero-pole-gain models

1. BACKGROUND AND INTRODUCTION

System identification has long been a focal point of research efforts at the DLR Institute of Flight Systems [1, 2]. Consequently several parameter estimation software packages were developed over the years, that could handle linear systems in the time and frequency domain as well as nonlinear systems and implemented output error, filter error and extended Kalman filter methods [3–6]. All of these software packages were written in FORTRAN.

When more and more research at the Institute was performed using MATLAB, it was desired to perform system identification directly in the MATLAB environment. This led to the development of the parameter estimation package FITLAB, that implemented maximum likelihood (ML) parameter estimation of nonlinear systems written in MATLAB.

Soon, FITLAB was equipped with a graphical user interface (GUI) to provide easy access to the standard tasks of reading the measured data, specifying the model and parameters, running the identification and looking at plots of the results. The software package was thus renamed into FitlabGui and over time it was enhanced by adding more model types (linear and polynomial models), a second optimization algorithm and the frequency response method as another identification algorithm.

Over the years, FitlabGui was merged with a data visualization tool and enhanced by an add-on package for helicopter handling qualities analysis based on [7]. Figure 1 shows the current range of functions of the software. The latest version of the FitlabGui software is described in [8, 9].

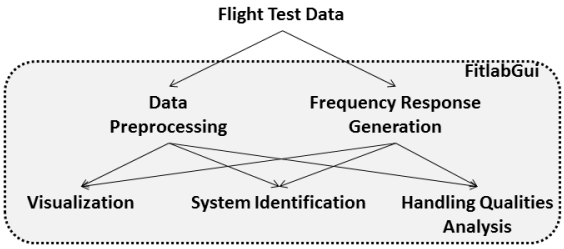

Figure 1: FitlabGui range of functions

FitlabGui requires at least MATLAB Version 7.5 and the control system toolbox.

The paper will first specify the supported data formats and list the routines that are available for data preprocessing. The further sections will describe the frequency response generation, the data visualization and analysis routines, the system identification options and the handling qualities analysis routines that are available for rotorcraft.

2. DATA HANDLING

2.1. Data Formats

FitlabGui allows to evaluate and analyze both time history and frequency response data.

For time history data, the supported file formats are R-CDF, MATLAB mat-files, ASCII and Excel files. R-CDF (Raw Common Data Format), the data format used for all current flight test programs at the Institute, is based on the Common Data Format [10] developed at the National Space Science Data Center (NSSDC) of NASA.

Time history data files that are not in one of the formats that are supported by FitlabGui can be imported via a user-written import routine.

Frequency responses (FRs) to be used in FitlabGui must be scalar LTI-objects (linear time-invariant systems) that are saved in mat-files. They can either be analytically defined or created from measured time history data. Analytically defined FRs/LTIs can be of type TF (transfer function) or ZPK (zero-pole-gain).

LTIs that contain measured frequency responses must be of type FRD (frequency response data) and the coherence can optionally be saved in the "Userdata" of the FRD-object. Frequency responses of the FRD type can be created from time domain data within FitlabGui (see section 3).

2.2. Data Preprocessing

A "Unit Conversion" option allows to rescale time history data, for example to remove sensor offsets or change data units. For the most commonly used conversions between different data units (e.g. angles from radians to degrees or vice versa), over 25 conversions are predefined.

More elaborate calculations than simple unit conversions can be performed using the so-called "Channel Arithmetic" (see figure 2). Using this option, data can for example be filtered or new signals can be calculated from measured ones.

Figure 2 shows an example where the body-fixed velocity components are calculated from airspeed, angle of attack and sideslip angle.

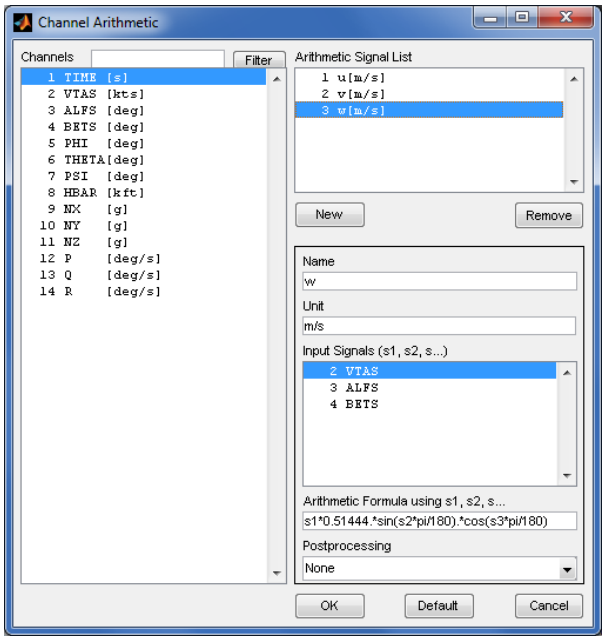

Figure 2: Channel Arithmetic panel

3. FREQUENCY RESPONSE GENERATION

A frequency response (FR) describes the response (magnitude and phase) to control input as a function of control input frequency and thus fully characterizes the dynamics of the complete input-to-output system. A FR is therefore often regarded as a nonparametric model. Frequency responses are a prerequisite for identification with the frequency response method (see section 5.1.2) and are also the basis for several handling qualities criteria.

FitlabGui offers three methods for FR generation that are described in the following subsections.

3.1. Frequency Response and Coherence

Let u_n and $y_n, n = 1, \cdots, N$ be the sampled input and output signals of the system under consideration. The length of the time interval is T and and the N data points are sampled with a sampling interval of Δt seconds , $T = \Delta t(N-1)$.

The corresponding finite Fourier transforms $U(f_k)$ and $Y(f_k)$ are determined at discrete frequencies $f_k = k/T = kf_1, \quad k = 0, \cdots, N-1$. The fundamental frequency or frequency resolution f_1 is the inverse of the length of the time interval. The Nyquist frequency $f_c = Nf_1/2 = (2\Delta t)^{-1}$ is the highest frequency available in the Fourier transform.

The auto-spectrum of the input signal is calculated from the Fourier transform by

$$G_{uu}(f_k) = \frac{2}{T}U^*(f_k)U(f_k) = \frac{2}{T}|U(f_k)|^2 \tag{1}$$

where $*$ denotes the conjugate complex value. An analogous equation holds for the output autospectrum. The cross-spectrum of the input/output signal is defined as

$$G_{uy}(f_k) = \frac{2}{T}U^*(f_k)Y(f_k) \tag{2}$$

and the frequency response H is now determined from

$$H(f_k) = \frac{G_{uy}(f_k)}{G_{uu}(f_k)}. \tag{3}$$

The coherence function γ^2_{uy} is an indicator of the correlation of the input and the output signals and is determined from

$$\gamma^2_{uy}(f_k) = \frac{|G_{uy}(f_k)|^2}{G_{uu}(f_k)G_{yy}(f_k)} \qquad 0 \le \gamma^2_{uy}(f_k) \le 1. \tag{4}$$

The standard technique for computing the discrete Fourier transforms is the Fast Fourier Transform (FFT). For the frequency response generation as implemented in FitlabGui, the Chirp-Z transform (CZT) is used instead of the FFT. Compared to the FFT, the CZT has the advantage that the frequency points, for which the Fourier transform shall be returned, can be specified (while still observing the limits of f_1 and f_c). This usually leads to a finer resolution of the FR in the frequency range of interest. Furthermore, the CZT allows to calculate the FT at the same frequency points when using time intervals of different lengths, which is necessary for the determination of composite frequency responses (see subsection 3.4). A description of the CZT can be found on pp. 393-399 of [11].

3.2. Windowing and Segmenting

The usual method to avoid frequency leakage is tapering or windowing of the data. (A good discussion of the phenomenon of frequency leakage can be found in [12] or [13].) In FitlabGui a Hanning window is used to process the input and output signals.

A frequency response as calculated from equation (3) exhibits a random error that manifests itself as scatter in magnitude and/or phase. This random error is caused by measurement noise in the output and unmeasured inputs (e.g. gusts). The random error of the FR can be reduced by segmenting, i.e. subdividing the data record into segments of equal size and then averaging over the results for the separate segments.

The random error ϵ_r is a function of the number of data segments n_d and of the coherence of the input/output relationship and is calculated by (see [12])

$$\epsilon_r\left(|H(f_k)|\right) = \frac{C_\epsilon\left[1-\gamma^2_{uy}(f_k)\right]^{1/2}}{|\gamma_{uy}|\sqrt{\frac{n_d+1}{2}}} \tag{5}$$

Here, C_ϵ is a constant that accounts for the degree of overlap between the segments (The numerical values for the two overlap percentages used in FitlabGui are $C_\epsilon = \sqrt{0.55}$ for 50% and $C_\epsilon = \sqrt{0.50}$ for 80% overlap).

If the data record of length N is subdivided into n_d segments that overlap by 50%, the segments each have a length of $M = 2N/(n_d+1)$. Because of the reduced length of the data segments compared to the full time interval, the fundamental frequency is increased to $f_1 = 1/(M\Delta t) = (n_d+1)/(2N\Delta t)$ Thus, by segmenting one has less error at the price of a coarser frequency resolution. (The Nyquist frequency, which depends solely on the sampling rate, is unchanged.)

The random error in equation (5) is normalized. Thus the standard deviation of the magnitude is

$$\sigma(|H(f_k)|) = \epsilon_r(|H(f_k)|)/|H(f_k)| \tag{6}$$

and the standard deviation of the phase is given by

$$\sigma(\angle(H(f_k))) = \sin^{-1}(\epsilon_r(|H(f_k)|)). \tag{7}$$

3.3. Multi-Input Single-Output Conditioning

When multiple inputs that are partially correlated excite one output, it is necessary to use multi-input / single-output (MISO) conditioning to arrive at meaningful frequency responses and coherence functions.

A system with two inputs u_1 and u_2 and one output y has the input/output relationship

$$Y = H_{1y}U_1 + H_{2y}U_2 \tag{8}$$

where H_{1y} and H_{2y} are the transfer functions between the first and second inputs and the output. If this equation is multiplied by U_1^* respectively U_2^*, it leads to

$$G_{1y} = H_{1y}G_{11} + H_{2y}G_{12} \tag{9}$$

$$G_{2y} = H_{1y}G_{21} + H_{2y}G_{22} \tag{10}$$

From these two equations, the conditioned frequency responses H_{1y} and H_{2y} are computed as

$$H_{1y} = \frac{G_{1y}\left[1 - \frac{G_{12}G_{2y}}{G_{22}G_{1y}}\right]}{G_{11}[1-\gamma_{12}^2]} = \frac{G_{1y,2}}{G_{11,2}} \tag{11}$$

$$H_{2y} = \frac{G_{2y}\left[1 - \frac{G_{21}G_{1y}}{G_{11}G_{2y}}\right]}{G_{22}[1-\gamma_{12}^2]} = \frac{G_{2y,1}}{G_{22,1}} \tag{12}$$

Here, $G_{1y,2}$, $G_{11,2}$, $G_{2y,1}$, and $G_{22,1}$ are the conditioned auto- and cross-spectra and γ_{12}^2 is the coherence between the two inputs u_1 and u_2 (cross control coherence)

$$\gamma_{12}^2 = \frac{|G_{12}|^2}{G_{11}G_{22}} \tag{13}$$

If the two inputs are totally uncorrelated, i.e. if $\gamma_{12}^2 = 0$, then the conditioned frequency responses reduce to the unconditioned ones.

For the analysis of frequency responses from partially correlated inputs, the ordinary coherence cannot be used. Instead the partial coherence has to be used, which is computed from the conditioned auto- and cross-spectra via

$$\gamma_{1y,2}^2 = \frac{|G_{1y,2}|^2}{G_{11,2}G_{yy,2}} = \frac{|G_{1y}G_{22} - G_{2y}G_{12}|^2}{G_{22}^2G_{11}G_{yy}(1-\gamma_{12}^2)(1-\gamma_{2y}^2)} \tag{14}$$

$$\gamma_{2y,1}^2 = \frac{|G_{2y,1}|^2}{G_{22,1}G_{yy,1}} = \frac{|G_{2y}G_{11} - G_{1y}G_{21}|^2}{G_{11}^2G_{22}G_{yy}(1-\gamma_{12}^2)(1-\gamma_{1y}^2)} \tag{15}$$

An extension of the determination of the conditioned auto- and cross-spectra and partial coherences to cases with more than two inputs can be found in [12] or [14]. In FitlabGui, the method described in [14] is used to determine the conditioned frequency responses.

3.4. Composite Frequency Responses

For larger segments, the minimum frequency f_1 is smaller, thereby yielding better results at the lower frequencies of interest. However, the corresponding lower number of segments available for averaging results in a higher random error ϵ_r, leading to increased oscillation of the magnitude and phase curves, especially at higher frequencies, where signal-to-noise ratios are generally lower. Smaller segments mean more averaging, which reduces the random error. This greatly improves the accuracy at higher frequencies, but at the expense of diminished information content at the lower frequencies of interest due to the higher minimum frequency.

The logical conclusion is that the optimal frequency response is a composite that is made up of several frequency responses with different numbers of segments (few segments at the low frequencies and many segments at higher frequencies). In FitlabGui two different methods for deriving composite frequency responses from the results for different segments are implemented.

The first method was developed by Ockier and is described in [15]. It is based on a weighting function that states that the frequency response derived by dividing the data record into n_d windows with 50% overlap is most trustworthy in the following frequency range

$$f_1\left[\left(\frac{n_d}{10}\right)^2 + 1\right] < f_k < f_1\left[\left(\frac{n_d}{10}\right)^2 + 1 + 14\frac{n_d}{10}\right] \tag{16}$$

This equation was developed empirically from helicopter response data obtained with frequency sweeps.

For the Ockier method, the computation of the composite frequency responses is performed with the following steps:

1. For each number of segments n_d, the data is segmented using 50% overlap and the frequency responses including MISO conditioning are computed and stored.
2. For each frequency point and each segmentation, the standard deviations of the amplitude and the phase are determined from equation (6) resp. equation (7).
3. For each segmentation, equation (16) is used to determine, which data points are trustworthy and which can be discarded.
4. For each frequency point that is to be considered, the optimal frequency response is computed by maximizing the likelihood of that data point. A Cauchy or Lorentzian distribution of the data (see chapter 15.7 of [16]) is assumed.

The second method was developed by Tischler and is described in chapter 10 of [17]. With this method, the conditioned spectra for n_w segmentations (usually up to 5) are used to derive composite spectra by minimizing a common cost function.

The weighting of the results for each segmentation is based on the corresponding random error (see equation (5)).

$$W_i = \left[\frac{(\epsilon_r)_i}{(\epsilon_r)_{min}}\right]^{-4} \qquad i = 1, \dots n_w \tag{17}$$

Thus the results with the lowest random error get a weighting of 1 and the other segmentations are deweighted.

The final composite spectra (index c) are those that minimize the following weighted least-squares cost function J for each frequency f:

$$\begin{aligned} J(f) = \sum_{i=1}^{n_w} W_i \Bigg\{ & \left(\frac{G_{uu_c} - G_{uu_i}}{G_{uu}}\right)^2 + \left(\frac{G_{yy_c} - G_{yy_i}}{G_{yy}}\right)^2 \\ & + \left(\frac{\Re(G_{uy_c}) - \Re(G_{uy_i})}{\Re(G_{uy})}\right)^2 \\ & + \left(\frac{\Im(G_{uy_c}) - \Im(G_{uy_i})}{\Im(G_{uy})}\right)^2 + 5\left(\frac{\gamma^2_{uy_c} - \gamma^2_{uy_i}}{\gamma^2_{uy}}\right)^2 \Bigg\} \end{aligned} \tag{18}$$

where $\Re(\dots)$ and $\Im(\dots)$ denote the real and imaginary part of the cross spectra. These composite spectra are then used to calculate the composite frequency response and coherence.

Including the coherence term in the cost function ensures that the coherence function of the composite frequency response will track the coherence of the most reliable windows over the entire frequency range. Due to the coherence term, the cost function depends nonlinearly on the desired composite spectral quantities and thus the cost function must be minimized iteratively.

For the Tischler method the computation of the composite frequency responses is performed with the following steps:

1. For each window length the spectra are computed using 80% overlap between the windows.
2. MISO conditioning is performed for all segmentations.
3. The weighting function from equation (17) is calculated for each segmentation.
4. Starting values for the composite results are determined by simple averaging.
5. For each frequency point the cost function from equation (18) is optimized to yield the composite spectra.
6. The composite frequency response and coherence are derived from the composite spectra.

3.5. Local Polynomial Method

Whereas segmenting and windowing has been a standard for frequency response calculation since the 1980s, the Local Polynomial Method (LPM) was developed at the end of the 2000s [18]. LPM is presented as an alternative to the windowing methods, with better performance due to an improved reduction of the leakage error. The performance of the LPM when applied to rotorcraft data is assessed in [19].

In contrast to the windowing methods, the LPM does not eliminate the leakage term through the application of windows, but it considers the leakage as an unknown function that has to be determined. Hence, the LPM assumes that the Fourier transforms U and Y of the input u and output y are linked by the so-called extended transfer function model

$$Y(k) = H(\omega_k)U(k) + L(\omega_k) + V(k) \tag{19}$$

for each frequency $\omega_k = 2\pi k f_s/N$ ($k = 1, ..., N$). Here f_s is the sampling frequency, N the number of samples, $H(\omega_k)$ the frequency response of the system, $L(\omega_k)$ the leakage term. $V(k)$ is the Fourier transform of the disturbing noise, which is assumed to be a filtered white noise.

The estimation of the frequency response with the LPM is based on the assumption that the FR $H(\omega)$ and the leakage $L(\omega)$ are smooth functions of frequency. Therefore, they can be approximated by complex polynomials within a narrow frequency band.

The LPM is available for both single-input / single-output (SISO) and multi-input / multi-output (MIMO) systems and is described in details in [18]. It has been shown in [20] that using concatenated data leads to a reduced bias and variance error of the frequency response estimate. The MIMO algorithm of the LPM can be used unchanged for concatenated data.

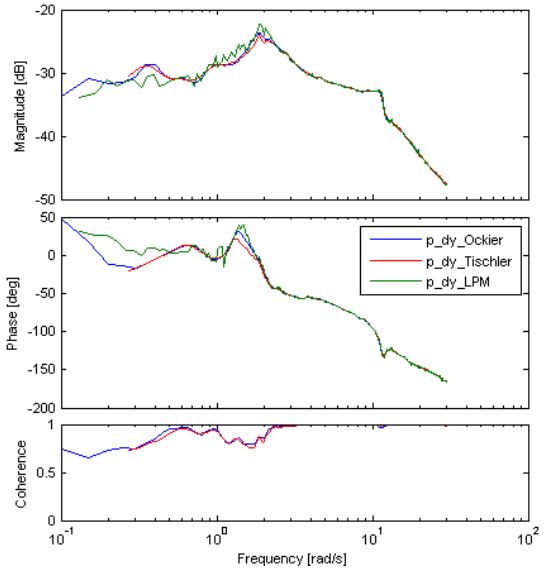

Figure 3: Frequency response p/δ_y for three methods

In general, the three implemented methods for FR generation yield similar results. This can be seen in figure 3 that shows the FR of roll rate p due to lateral cyclic input δ_y for the three implemented methods. Differences occur mainly at the lower frequencies.

The LPM performs better for resonance phenomena but does not give coherence information. Tischler's method yields auto and cross spectra as well as the random error in addition to the FR and coherence.

Once frequency responses have been generated in FitlabGui, they can be inspected via Bode plots and saved as FRD objects in mat-files so they can later be used for modeling or HQ analysis.

4. DATA VISUALIZATION AND ANALYSIS

FitlabGui provides the following plots to visualize the measured data and to illustrate the identification results:

- Quick Plot Time Domain
- Report Plot Time Domain
- Cross Plot
- Quick Bode Plot
- Report Bode Plot
- Spectral Plot
- Mismatch Envelope Plot
- Quick Plot Frequency Domain
- Report Plot Frequency Domain

The first three plots work on time domain data, whereas the next four plots work on frequency response data. The last two plots use data that are Fourier transformed from the time domain into the frequency domain. All time domain plots support displaying data from several time intervals in one plot.

4.1. Time History Data

The "Quick Plot Time Domain" produces a stripchart plot of the concatenated data from all time intervals that can be used for quick inspection of the test data. If data from only one maneuver is plotted, the data can be displayed versus the original measured time values. Otherwise, an artificial time axis is generated.

More elaborated plots, that allow up to four channels per diagram and several plot pages with up to nine diagrams per page, are created with the "Report Plot Time Domain". Once a simulation or an identification has been performed, this plot type also allows to create plots that compare the model outputs with the corresponding measured signals. Furthermore, the errors between the model output and the measured output variables are available as additional signals and thus can be plotted also.

Figure 4 shows an example of a report plot that allows to assess the match between an identified engine model and the measured data for four time intervals. The first diagram shows the measured collective and pedal control inputs for the different 3211-multistep maneuvers. The second diagram shows the match between the measured rotor speed and the model output Ω and the last diagram displays the remaining rotor speed error.

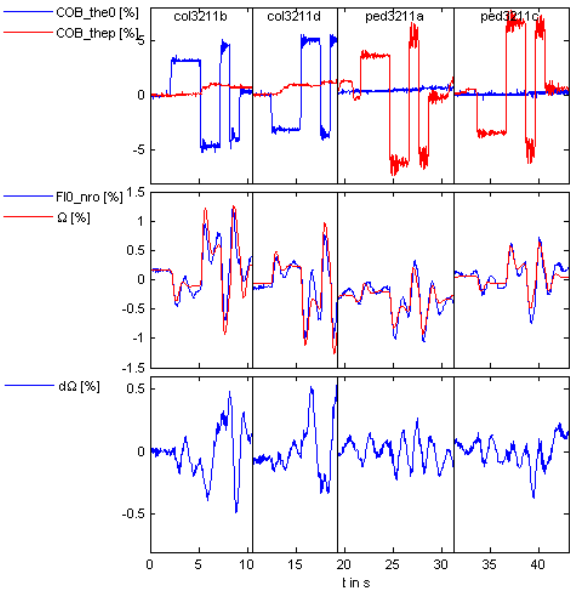

Figure 4: Report plot: Match of identified engine model

The "Cross Plot" allows to plot up to 10 pairs of channels. Each curve can be approximated by a regression of up to 3rd order.

Figure 5 is an example from the noseboom calibration effort for the ACT/FHS helicopter. Shown is Δp_s, the difference in static pressure between the uncalibrated noseboom values and the calibrated values from the on-board airdata system, versus true airspeed. Δp_s as an approximation for the noseboom position error is expected to be proportional to the dynamic pressure or to the square of the airspeed. Therefore, a 2nd order regression curve was calculated.

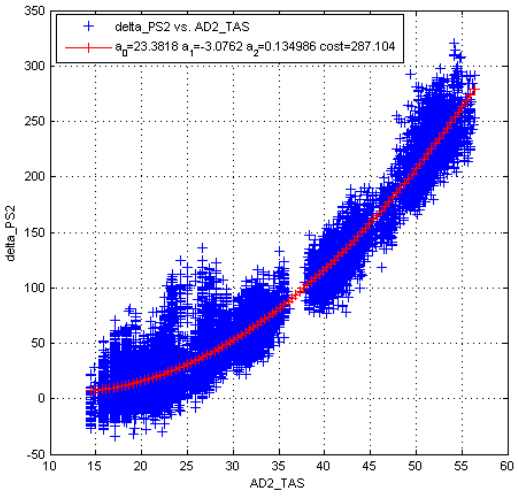

Figure 5: Cross plot of position error versus airspeed

4.2. Frequency Response Data

For frequency responses, the "Quick Bode Plot" allows to create Bode plots with the amplitude in dB and the phase in radians or degrees versus frequency on a semilog scale. If the frequency responses have a coherence, it can be displayed in a third diagram below the amplitude and phase. Figure 3 is an example for such a plot.

The "Report Bode Plot" allows to define several plot pages where each page can contain up to six frequency response diagrams with up to four frequency responses in each diagram. Once a simulation or identification with the frequency response method has been performed, all measured and calculated frequency responses are available for plotting.

An example for such a plot, illustrating the on-axis match of an identified 6-DoF model for the ACT/FHS, is shown in figure 6. The upper diagrams show the match for pitch rate due to longitudinal cyclic (q/δ_x) and roll rate due to lateral cylic input (p/δ_y). The bottom diagrams illustrate the match for yaw rate due to pedal (r/δ_p) and vertical acceleration due to cyclic input (a_z/δ_0).

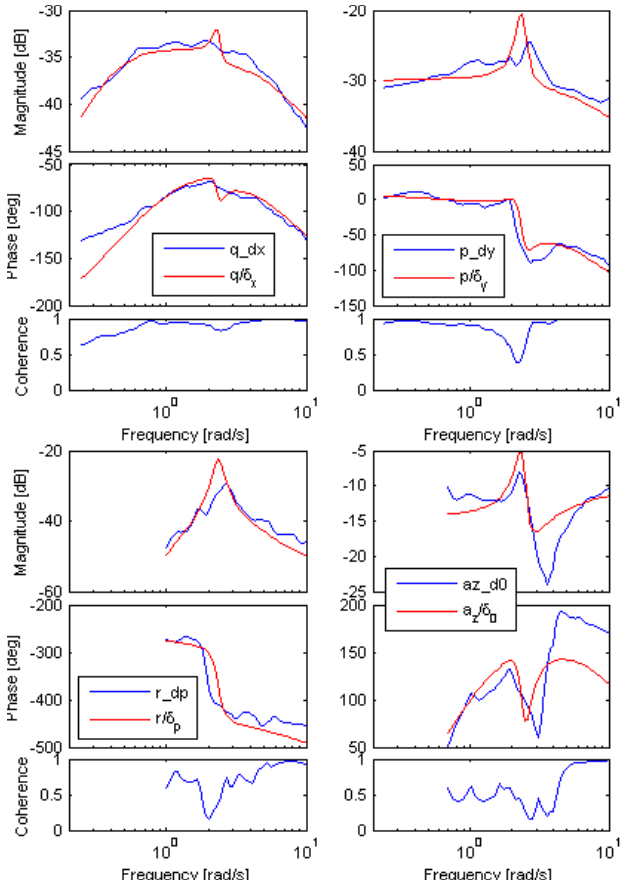

Figure 6: On-axis match of 6-DoF model (120 kts)

If frequency responses were generated with Tischler's method, the input and output spectra, the cross spectrum and the random error are saved in addition to amplitude, phase and coherence of the frequency response. The "Spectral Plot" then allows to plot and analyze all of this information.

In the fixed-wing military handling qualities criteria standard MIL-STD-1797 [21], mismatch criteria have been defined to evaluate the match between an actual frequency response and its low-order equivalent system model. The boundaries correspond to limits on the maximum unnoticable added dynamics (MUAD), beyond which a pilot will detect a deviation in the response characteristics.

A plot showing the approximation errors in comparison to these limits can be created with the "Mismatch Envelope Plot". An example for such a plot is shown in figure 7.

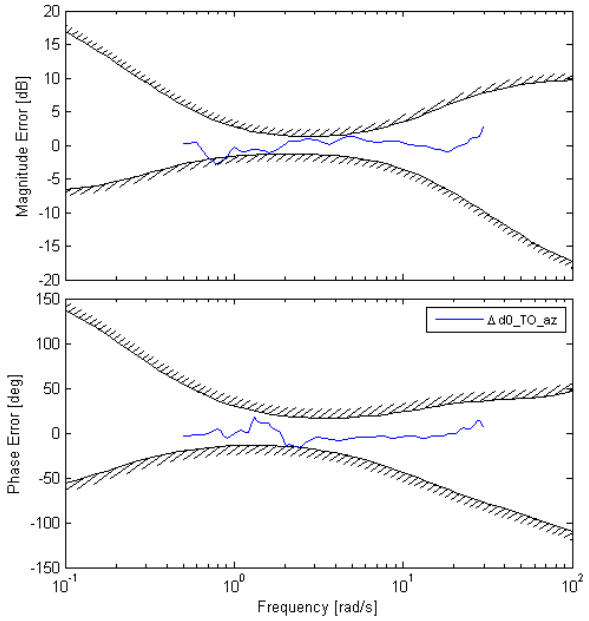

Figure 7: Mismatch envelope plot

4.3. Fourier-Transformed Data

The maximum likelihood (ML) identification method in the frequency domain matches the Fourier transforms of the system outputs. Fourier transforms of measured data can be plotted with the "Quick Plot Frequency Domain". For each signal, an amplitude diagram and a phase diagram is generated.

The "Report Plot Frequency Domain" allows to display the same type of frequency domain data on several plot pages with up to four diagrams each. Once a frequency domain identification with the ML output error method has been performed, this plot type allows to illustrate the match between the measured outputs and the model outputs in the frequency domain.

5. SYSTEM IDENTIFICATION

System identification is an iterative model building process to obtain an accurate mathematical description from measured system responses. Depending on the system to be modeled and the complexity of the desired model, different methods and model structures are appropriate. A good overview of time domain system identification is given in [22] whereas all aspects of frequency domain identification are covered in [17].

5.1. Methods

Two identification methods are implemented in FitlabGui, namely the Maximum Likelihood (ML) Output Error Method and the Frequency Response Method. Both are described in the next subsections.

5.1.1. Maximum Likelihood Method

The dynamical system whose parameters are to be estimated is assumed to be described by the following mathematical model:

$$\begin{aligned} \dot{x}(t) &= f\left[x(t), u(t), \varphi\right]; \qquad x(t_0) = x_0 \\ y(t) &= g\left[x(t), u(t), \varphi\right] \end{aligned} \tag{20}$$

Here, x and u denote the state and control input vectors. The model structure (f, g) is given and the coefficients φ and the initial conditions x_0 form the vector θ of the unknown parameters.

Measurements z of the output variables that are corrupted with noise v exist for N discrete sampling times t_k.

$$z(t_k) = y(t_k) + v(t_k); \qquad k = 0, \ldots, N-1 \tag{21}$$

It is assumed that the state and observation equations correctly describe the dynamic system, i.e. that no modeling errors are present. The measurement errors are usually assumed to be characterized by stationary zero-mean Gaussian white noise with covariance matrix R.

The ML estimates of the unknown parameters θ and the noise covariance matrix R are obtained by the following cost function

(22)

$$J(\theta, R) = \frac{1}{2} \sum_{k=0}^{N-1} \left[z(k) - y(k)\right]^T R^{-1} \left[z(k) - y(k)\right] + \frac{N}{2} \log(\det(R))$$

The optimization of this cost function J is carried out in two steps. In the first step, it can be shown that for any given value of θ, the ML estimate of R is given by

$$\hat{R} = \sum_{k=0}^{N-1} \left[z(k) - y(k)\right] \left[z(k) - y(k)\right]^T \tag{23}$$

This means that the output error covariance matrix is the most plausible estimate for R.

With this estimate for R, the first term of J reduces to a constant and the variable part reduces to the determinant of the covariance matrix

$$J = \det(R) \tag{24}$$

In FitlabGui, R is implemented as a diagonal matrix. This means that the measurement errors are assumed to be uncorrelated. The cost function J then reduces to the product of the output error variances of all m output variables.

$$J = \prod_{i=1}^{m} \sigma^2(z_i - y_i) \tag{25}$$

with

$$\sigma^2(z_i - y_i) = \frac{1}{N} \sum_{k=0}^{N-1} \left[z_i(t_k) - y_i(t_k)\right]^2 \tag{26}$$

As shown in [3], this also leads to faster convergence of the identification.

The Maximum Likelihood cost function in the frequency domain is derived analogously as

(27)

$$J(\theta, S) = \frac{1}{2} \sum_{k=1}^{N_\omega} \left[Z(\omega_k) - Y(\omega_k)\right]^* S^{-1} \left[Z(\omega_k) - Y(\omega_k)\right] + \frac{N_\omega}{2} \log(\det(S))$$

where Z and Y are the Fourier transforms of the measured and calcuated outputs and S is the spectral density matrix of the measurement noise. Optimization of this cost function is performed in the same way as in the time domain case.

5.1.2. Frequency Response Method

In the previous subsection, frequency domain identification based on matching the Fourier transforms of the measured time histories has been described. Another method, the frequency response method, is based on matching the frequency responses.

The quadratic cost function J to be minimized for the frequency response method is

$$J = \frac{20}{N_\omega} \sum_{k=1}^{N\omega} w_\gamma(k) \Big[\left(|H_m(k)|_{dB} - |H(k)|_{dB}\right)^2 + w_{ap} \left(\angle H_m(k) - \angle H(k)\right)^2 \Big] \tag{28}$$

where N_ω is the number of frequency points in the frequency interval $[\omega_1, \omega_{N\omega}]$. H_m is the frequency response

of the data to be approximated (either generated from measured time history data as described in section 3 or analytically generated in the case of a given high-order system). H is the frequency response of the model. $|.|_{dB}$ is the amplitude in dB and $\angle(.)$ the phase in deg.

w_{ap} is the relative weighting between amplitude and phase errors. The normal convention is $w_{ap} = 0.01745$ and this value is the default used in FitlabGui. The military standard on flying qualities [21] suggests a value of $w_{ap} = 0.02$.

w_γ is an optional weighting function based on the coherence between the input and the output at each frequency. If coherence data are available and if coherence weighting is used, then

$$w_\gamma(k) = \left[1.58(1 - e^{\gamma^2_{xy}(k)})\right]^2, \tag{29}$$

otherwise $w_\gamma \equiv 1$. This is the same weighting function as used in CIFER® [17].

When several frequency responses are approximated together, the overall cost function is the average of the individual cost functions. Due to this fact and because the amplitude and phase errors always have the same scaling, the absolute value of the cost function from equation (28) is a direct measure of the goodness of fit. According to [17], a cost function of $J \leq 100$ usually yields an acceptable level of accuracy for flight dynamics modeling.

The frequency response method can be used to approximate frequency responses that were derived from measured time histories of the input and output variables. The method can also be used to approximate an analytically derived high-order model by a low-order equivalent system.

5.2. Model Interfaces

FitlabGui allows for the identification of the following model types:

- nonlinear models
- linear models
- polynomial transfer function models

Nonlinear and linear models must be specified by the user in model files. Polynomial models are directly specified in a panel.

5.2.1. Nonlinear Models

A nonlinear user model is an m-file that has to provide the model output y for one maneuver as a function of the unknown parameters φ, the initial conditions x_0 and optionally other bias parameters of the current maneuver, the time axis t and the measured input u. The integration of the state equations is thus in the responsibility of the user.

Nonlinear models can contain calls to Simulink models which enables the identification of parameters within Simulink models.

Complicated models in combination with large datasets often lead to long computation times. Therefore, the latest version of FitlabGui allows nonlinear models to also be specified as C^{++}-code. If a user model is specified as C^{++}-code, FitlabGui automatically uses a parallelized version of the sensitivity equations in the optimization with the Gauss-Newton method (see subsection 5.3) which further speeds up the computation.

System identification with FitlabGui using nonlinear models has been performed for a wide variety of vehicles including modeling of the reusable launch vehicle Phoenix [23], identification of a parafoil [24, 25], flight path reconstruction and noseboom calibration of the ACT/FHS [26], identification of a gyrocopter simulator model [27, 28], modeling of the SB-10 sailplane including flexible modes [29], determination of a UCAV (Unmanned Combat Aerial Vehicle) model from dynamic wind tunnel tests [30], identification of wake vortex models [31] and modeling of icing effects for a light business jet [32].

5.2.2. Linear Models

If the system state and observation functions are linear in the state and control variables, a different model is suitable. By substituting the state and control input variables with their deviations from the initial condition, the model equations 20 are transformed into

$$\begin{aligned} \dot{x}(t) &= A(\varphi) \cdot x(t) + B(\varphi) \cdot u(t) + b_x;\ x(t_0) = 0 \\ y(t) &= C(\varphi) \cdot x(t) + D(\varphi) \cdot u(t) + b_y \end{aligned} \tag{30}$$

In this linear model, b_x and b_y are the lumped bias parameters of the state and observation equations respectively. They are linear combinations of the original initial conditions and zero-offsets in the input and output variables. All components of b_x and b_y can be estimated if the system is observable. If necessary, the model can be extended by input and/or output time delays τ.

For the identification of linear models with FitlabGui, the user has to provide a model m-file that calculates the system matrices A, B, C, D and optionally the bias vectors b_x, b_y and the time delay τ as a function of the unknown parameters. The integration of the state equations and calculation of the output equations respectively the calculation of the transfer functions of the model is done by FitlabGui using routines from the MATLAB control system toolbox.

Examples for system identification projects using linear models include the identification of the miniature helicopter ARTIS [33] and the ACT/FHS helicopter [34–37] as well as the identification of pilot models [38, 39].

5.2.3. Polynomial Transfer Function Models

A transfer function model F can be specified by numerator and denominator polynomials

(31)

$$F(s) = \frac{b_m s^m + b_{m-1} s^{m-1} + \ldots + b_1 s + b_0}{a_n s^n + a_{n-1} s^{n-1} + \ldots + a_1 s + a_0} \, e^{-\tau s}$$

This model has to be made unique by either setting a_n or a_0 to 1. In the model, τ is an equivalent time delay that can be used to account for unmodeled higher order dynamics.

Alternatively, the transfer function can also be displayed in the factored form with poles and zeros.

(32)

$$F(s) = k \frac{(s - z_1)(s - z_2) \ldots (s - z_m)}{(s - p_1)(s - p_2) \ldots (s - p_n)} \, e^{-\tau s}$$

Here, z_i and p_i respectively denote the zeros and poles of the transfer function and k is the gain.

If the zeros or poles are complex conjugate pairs, they are usually displayed in terms of the damping ratio ζ and natural frequency ω_n as

$$[\zeta, \omega_n] \Leftrightarrow [s^2 + 2\zeta\omega_n s + \omega_n^2]$$

Pole/zero models are more convenient when the approximate location of at least some of the poles and/or zeros is known and bounds can be placed on the corresponding parameters.

In FitlabGui both model types (numerator/denominator and pole/zero) can be used in the specification of transfer function identification models and automatic transformation between the two variants is provided. Several frequency responses can be approximated together, if the corresponding transfer function models have the same denominator.

Within FitlabGui, polynomial models are easily defined via the panel shown in figure 8. The identification of polynomial models that are defined this way is only possible with the frequency response method. For identification with the (time or frequency domain) ML method, the polynomial model would have to be converted into a linear model.

Application examples for polynomial models include turbulence modeling [34, 40], modeling of sidestick dynamics [41] and identification of pilot models [39].

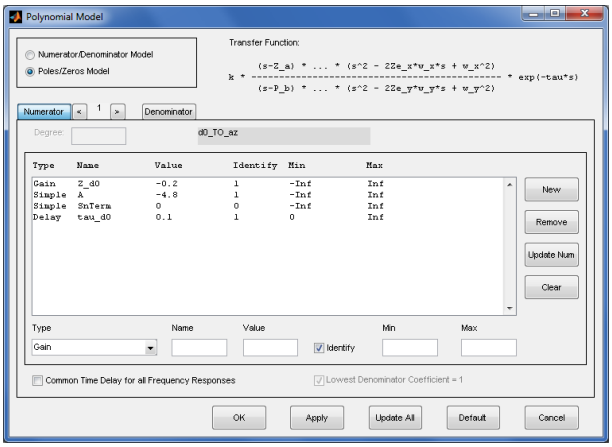

Figure 8: Panel for definition of polynomial models

5.3. Optimization

Adjusting the model parameters so that they minimize the cost function from equations (22), (27) or (28) is an optimization problem.

The optimization method most widely used for parameter estimation is the Gauss-Newton method where, starting from an initial guess, the parameters are obtained iteratively. In each iteration, a system of linear equations for the parameter improvement has to be solved. The Gauss-Newton method gives information about the accuracy and the correlation of the parameter estimates. The Gauss-Newton method as implemented in FitlabGui is enhanced by a line search algorithm for improved performance and allows for parameter bounds [42].

For systems with discontinuities, gradient-based optimization methods like the Gauss-Newton method usually fail and simplex-based methods are used instead. The standard Simplex algorithm [43] for the case of n unknown parameters starts with an n-dimensional simplex formed by $n + 1$ points in the parameter space. Iteratively, the worst point is replaced by a better point through reflection, expansion, or contraction of the simplex. The algorithm ends when all points are close to each other.

The standard Simplex algorithm works well for problems with few unknowns but often fails for more than five unknown parameters. Thus, the Subplex algorithm developed by Rowan in [44] is implemented in FitlabGui. The Subplex algorithm subdivides the problem space into orthogonal subspaces of lower dimension (between 2 and 5) and then uses the Simplex algorithm on these subspaces. The main subspace is chosen such that the direction of largest improvement from the last iteration step is included in this subspace. More details about the Subplex algorithm can be found in [44, 45].

The basic Simplex and Subplex algorithms do not account for parameter bounds. In [46] a method for considering bounds in the Simplex algorithms is presented. This approach has been successfully integrated into the Subplex algorithm as used in FitlabGui [45].

For both methods, the optimization process is stopped when either the relative change of the cost function or the relative change of the unknown parameters from one iteration to the next is smaller than a specified limit or when the specified maximum number of iterations is reached.

6. HELICOPTER HQ ANALYSIS

Helicopter handling qualities requirements are specified in the Aeronautical Design Standard ADS-33 [47]. They consist of quantitative requirements that evaluate the response to prescribed inputs and qualitative criteria that are implemented through a set of demonstration maneuvers or Mission Task Elements (MTEs).

6.1. Quantitative Criteria

The quantitative criteria from the ADS-33 are divided into small-, mid- and large-amplitude as well as into short-term and mid-term criteria. Requirements are specified for the on-axis responses in pitch, roll, yaw and heave as well as for the inter-axis coupling responses. The limits for the quantitative parameters are usually a function of the Usable Cue Environment (UCE), the pilot attention state (full or divided attention), the helicopter response type (rate or attitude command) and the required degree of agility (limited, moderate, aggressive agility and TAT (target acquisition and tracking)). Separate requirements exist for the hover/low speed and the forward flight regime.

FitlabGui allows to evaluate the following quantitative handling qualities criteria that are defined in the ADS-33:

- Bandwidth
- Dynamic Stability
- Attitude Quickness
- Large Amplitude
- Spiral Stability
- Height Response
- Torque Response
- Pitch due to Collective
- Yaw due to Collective
- Pitch-Roll Coupling
- Roll-Sideslip Coupling

The first five criteria pertain to the pitch, roll, and yaw motion whereas the next two criteria pertain to the vertical motion. The last four criteria are coupling criteria.

Depending on the specific criterion, the quantitative criteria work on time domain and/or frequency response data. The handling qualities routines are fully integrated into FitlabGui. That means that all data that have been loaded into FitlabGui are available for HQ analysis.

Handling qualities analysis, using the same routines that now have been included in FitlabGui, was performed for the CH-53G [48, 49].

6.1.1. Bandwidth

The bandwidth criterion addresses small-amplitude short-term attitude changes due to a control input. The criterion parameters bandwidth ω_{BW} and phase delay τ_p are determined from the frequency response of attitude due to control input as defined in figure 6 of ADS-33 [47]. The user has to specify the current axis (pitch, roll, or yaw), the speed (hover or forward flight), the command system type (rate or attitude command) and the frequency responses to be evaluated (see figure 9).

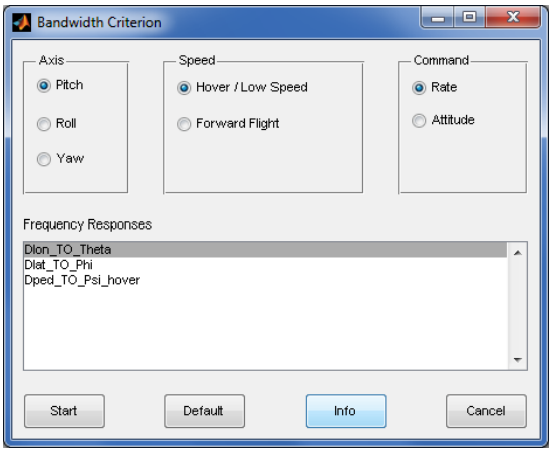

Figure 9: Panel for bandwidth criterion

First, the 180°-crossing that corresponds to the neutral stability frequency ω_{180} has to be selected. Once ω_{180} has been determined, the gain bandwidth $\omega_{BW_{gain}}$ (frequency at which the gain margin is 6 dB) and phase bandwidth $\omega_{BW_{phase}}$ (frequency at which the phase margin is 45°) are determined automatically. The bandwidth and phase delay are then calculated via

(33)
$$\omega_{BW} = \begin{cases} \min\left(\omega_{BW_{gain}}, \omega_{BW_{phase}}\right) & \text{rate response} \\ \omega_{BW_{phase}} & \text{attitude response} \end{cases}$$

and

(34)
$$\tau_p = \frac{\Delta\Phi_{2\omega_{180}}}{\frac{360}{2\pi}(2\omega_{180})}$$

where $\Phi_{2\omega_{180}}$ is the difference in phase angle between ω_{180} and $2\omega_{180}$.

6.1.2. Dynamic Stability

The dynamic stability criterion is a classical stability criterion that examines mid-term small-amplitude attitude changes due to a control input. The criterion metrics are the natural frequency ω_n and damping ratio ζ of the oscillatory modes. The dynamic stability criterion is applicable at all frequencies below the bandwidth frequency in pitch and at all frequencies for the other axes and thus addresses the phugoid and Dutch roll modes.

The determination of the dynamic stability parameters from time history data is only possible if the phugoid and Dutch roll responses are separated which is usually only the case

in forward flight. Then, the eigenmotions can be excited by a pulse or doublet in longitudinal cyclic (lateral cyclic, pedal) input and the natural frequency and damping ratio can be determined either by the logarithmic decrement method or by fitting a decreasing sinusoidal function to the response.

6.1.3. Attitude Quickness

The attitude quickness criterion evaluates the response to aggressive control inputs with moderate amplitudes and thus yields the connection between the bandwidth and the large amplitude criteria. The criterion shows how fast the helicopter is able to transition from one stationary attitude to another stationary attitude without large pilot corrections.

The criterion assumes the response characteristics to be those of a second order system. The parameters of the criterion are the attitude quickness, defined as the ratio of the maximum angular rate to the peak attitude change and the minimum attitude change during transition from one attitude to another. Peak attitude change, minimum attitude change and peak angular rate have to be marked by the user in the corresponding diagrams.

Figure 10 shows an example for a roll-axis analysis plot where the calculated quickness parameters (maximum roll rate p_{pk}, peak and minimum roll attitude change $\Delta\Phi_{pk}$ and $\Delta\Phi_{min}$) are shown in comparison the HQ levels from the ADS-33.

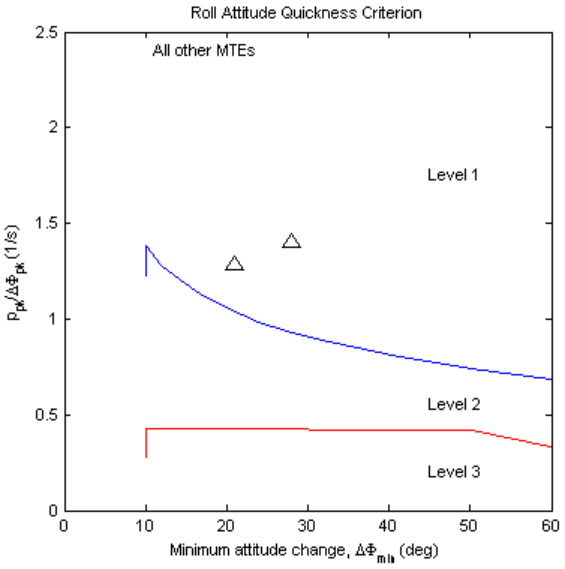

Figure 10: Example for roll attitude quickness results plot

6.1.4. Large Amplitude

This criterion addresses large-amplitude changes in attitude and measures the absolute control power in terms of the maximum achievable angular rate (for rate response types) or maximum achievable attitude change from trim (for attitude response types).

For the yaw response in forward flight, the criterion parameter changes to the achievable heading change within one second following an abrupt pedal step input.

Starting the evaluation initiates a plot of control input, angular rate and attitude angle. The maximum angular rate resp. the maximum angular attitude change is determined automatically and marked in the plot.

For the yaw response in forward flight, the initial time of the step input has to be determined first which can either be done automatically or manually by the user. Once the initial time has been determined, the heading change within one second is determined automatically.

6.1.5. Spiral Stability

The spiral stability criterion allows helicopters to have a slightly unstable spiral mode in forward flight. Limits are given for the time to double of the bank angle amplitude following a lateral pulse control input.

A method for determining the time to double T_2 is given in [50]. The time response of the bank angle response has to be plotted on a semilog scale. The spiral component is then the time-averaged response after the first few seconds where the roll and Dutch roll modes still dominate the response. As long as there are no nonlinearities in the response, the spiral is well approximated by a straight line drawn through the time history after the initial response. The time to double is then determined as

$$T_2 = \ln 2 \, \frac{-(t_2 - t_1)}{\ln(\hat{\phi}_2/\hat{\phi}_1)} \tag{35}$$

where $\hat{\phi}_1$ and $\hat{\phi}_2$ are values of the linear approximation of the bank angle curve at times t_1 and t_2.

6.1.6. Height Response

The height response criterion is aimed at measuring the dynamic behavior following collective inputs - in particular the vertical damping and equivalent vertical axis time delay.

The ADS-33 requirement for the vertical response in hover is based on the premise that the altitude rate responds to collective inputs as a first order system for at least five seconds following a step collective input [47]. This first order system is defined by the transfer function

$$\frac{\dot{h}}{\delta_0} = \frac{K e^{-\tau_{\dot{h}_{eq}} s}}{T_{\dot{h}_{eq}} s + 1} \tag{36}$$

where K is the gain, $\tau_{\dot{h}_{eq}}$ is the equivalent time delay of the system (to account for actuation and rotor dynamics) and $T_{\dot{h}_{eq}}$ is the equivalent time constant. The handling qualities requirements are formulated in terms of the time constant and the time delay.

The ADS-33 [47] states that the equivalent system parameters shall be obtained by a time domain least squares fit of the function

$$\dot{h}_{est}(t) = K\left(1 - e^{-\frac{t-\tau_{h_{eq}}}{T_{h_{eq}}}}\right) \tag{37}$$

to the five seconds of vertical rate response following the collective step input. The coefficient of determination

$$r^2 = \frac{\sum_{i=1}^{n}\left(\dot{h}_{est}(t_i) - \dot{h}_{mean}\right)^2}{\sum_{i=1}^{n}\left(\dot{h}(t_i) - \dot{h}_{mean}\right)^2} \tag{38}$$

with

$$\dot{h}_{mean} = \frac{1}{n}\sum_{i=1}^{n}\dot{h}(t_i)$$

shall be in the range $0.97 < r^2 < 1.03$ for the fit to be valid. This method does not use the actual collective control input but assumes that a perfect step input was used.

Alternatively, a time domain fit using a simulation with the transfer function from equation (36) and the measured collective control input can be performed to obtain the criterion parameters $T_{\dot{h}_{eq}}$ and $\tau_{\dot{h}_{eq}}$. This method was developed at DLR [51] and uses the measured control input and thus can handle non-perfect step inputs. The coefficient of determination is again calculated from equation (38).

Another alternative way for evaluating this criterion is a transfer function fit in the frequency domain as suggested by Ockier in [51]. This method needs frequency response data for altitude rate due to collective input $\dot{h}/\delta_0$ that is usually derived from a collective frequency sweep.

In FitlabGui, all the above described methods for evaluating the height response criterion are implemented. Figure 11 shows the corresponding panel.

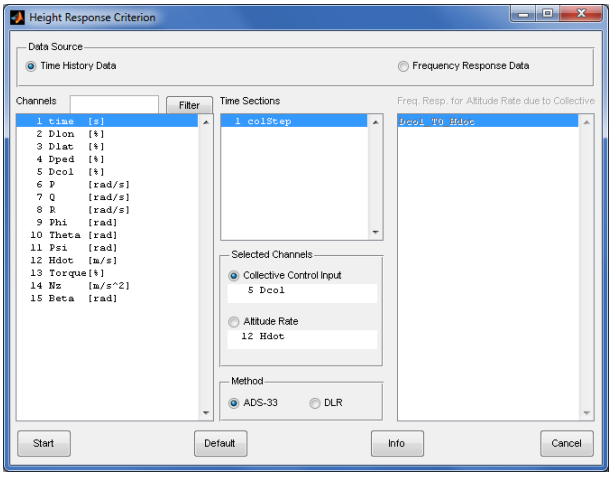

Figure 11: Height response criterion panel

6.1.7. Torque Response

The torque response criterion uses the torque displayed to the pilot as a measure of the maximum allowable power that can be commanded without exceeding engine or transmission limits.

The criterion imposes limits on the time t_p at which the peak of torque Q_0 occurs and the amount of torque overshoot Q_0/Q_1. Here, Q_1 is the first torque minimum occuring within ten seconds of the initiation of the collective step input. If no torque minimum is present within these ten seconds, Q_1 is taken as the torque at 10 seconds.

6.1.8. Pitch Due to Collective

The pitch due to collective criterion in forward flight places limits on the pitch attitude change occurring within three seconds of an abrupt change in collective. The amount of pitch angle change is weighted against the amount of normal acceleration n_z that is generated by the collective input. The criteria limits are expressed in terms of the peak pitch angle to peak normal acceleration ratio $|\theta_{pk}/n_{z_{pk}}|$.

Upon starting the evaluation, a time history plot is drawn and the step initial time is selected automatically or manually. Once the step initial time has been determined, the peak normal acceleration and peak pitch attitude are determined automatically.

6.1.9. Yaw Due to Collective

The yaw due to collective criterion limits the yaw rate response to abrupt collective inputs with the directional controls fixed. The criterion is specified in terms of two parameters, a mid-term response parameter $r_3/|\dot{h}(3)|$ and a short-term response parameter $|r_1/\dot{h}(3)|$.

r_1 is the peak yaw rate which occurs in the first three seconds after the collective input or, if there is no obvious peak yaw rate, the yaw rate one second after the collective input. r_3 is the yaw rate change between the first and the third second after the input (between $r(1)$ and $r(3)$). The sign of r_3 is positive if $r(1)$ and $r(3)$ have the same sign (i.e. the yaw rate change is continuous) and negative if $r(1)$ and $r(3)$ have different signs (i.e. the yaw rate change is oscillatory in nature). $\dot{h}(3)$ is the rate of climb or descent measured three seconds after the collective input.

After starting the evaluation, a time history plot appears and the step initial time has to be detected either automatically or manually. Then, the user is asked whether the peak yaw rate occurs within three seconds of the step input. Depending on the answer, the peak yaw rate or the yaw rate after one second is determined automatically and the criterion parameters are calculated.

6.1.10. Pitch-Roll Coupling

The ADS-33 criteria for roll-to-pitch (i.e. pitch due to roll) and pitch-to-roll (i.e. roll due to pitch) coupling are defined in the time domain for agressive agility and in the frequency domain for target aquisition and tracking.

The time domain requirements are defined in terms of the ratio of the peak off-axis attitude response to the desired on-axis response, i.e. $\Delta\theta_{pk}/\Delta\phi_4$ for roll-to-pitch and $\Delta\phi_{pk}/\Delta\theta_4$ for pitch-to-roll coupling. The peak off-axis response must be measured within four seconds following an abrupt longitudinal or lateral cyclic step input; the desired on-axis response must be measured exactly four seconds after the input.

The frequency domain requirements are defined in terms of the average pitch-due-to-roll (q/p) and roll-due-to-pitch (p/q) that are derived from ratios of pitch and roll frequency responses. The average q/p is defined as the magnitude of pitch-due-to-roll control input (q/δ_y) divided by roll-due-to-roll control input (p/δ_y) averaged between the bandwidth and neutral-stability (phase = -180°) frequencies of the pitch-due-to-pitch control inputs (q/δ_x). Analogously, average p/q is defined as the magnitude of p/δ_x divided by q/δ_x between the roll-axis p/δ_y bandwidth and neutral stability frequencies.

For the time domain criterion, the step initial time has to be defined either automatically or manually. The peak off-axis response and the on-axis response after four seconds are calculated automatically.

For the TAT cases that are evaluated in the frequency domain, four frequency responses (q/δ_x, p/δ_x, q/δ_y, p/δ_y) have to be specified for each case. Once the evaluation is started, bode plots for the on-axis responses θ/δ_x (integrated from q/δ_x) and ϕ/δ_y (integrated from p/δ_y) appear, where the user has to select the correct 180°-crossing for the bandwidth calculation. After the bandwidth and neutral stability frequencies have been determined, the criterion parameters are calculated automatically.

6.1.11. Roll-Sideslip Coupling

The roll-sideslip coupling criterion places requirements on the amount of coupling that can exist between roll and sideslip for moderate bank angle change maneuvers such as turn entry. The way in which roll-sideslip coupling manifests itself is mainly a function of two parameters, the ratio of the amplitudes of the bank angle and sideslip angle envelopes of the Dutch roll mode, $|\phi/\beta|_d$, and the phase angle ψ_β of the Dutch roll oscillation in sideslip following a lateral cyclic input.

The roll-sideslip criterion consists of two requirements: a limit on bank angle oscillations, and a limit on sideslip excursions during turn coordination. The bank angle oscillation limit is formulated through the ratio of the amount of Dutch roll oscillation versus the mean bank angle ϕ_{OSC}/ϕ_{AV} This ratio is determined as

(39)
$$\frac{\phi_{OSC}}{\phi_{AV}} = \begin{cases} \frac{\phi_1+\phi_3-2\phi_2}{\phi_1+\phi_3+2\phi_2} & \zeta_d \le 0.2 \\ \frac{\phi_1-\phi_2}{\phi_1+\phi_2} & \zeta_d > 0.2 \end{cases}$$

where ϕ_1, ϕ_2 and ϕ_3 are the bank angles at the first, second and third peaks following an impulse lateral cyclic input and ζ_d is the damping ratio of the Dutch roll oscillation.

The phase angle ψ_β is determined as

(40)
$$\psi_\beta = \frac{360 t_{1\beta}}{T_d} \quad \text{with} \quad T_d = \frac{2\pi}{\omega_d\sqrt{1-\zeta_d^2}}$$

where T_d and ω_d are the period and the natural frequency of the Dutch roll and $t_{1\beta}$ is the time to the first sideslip peak.

In FitlabGui, the Dutch roll frequency and damping (ω_d, ζ_d) are first determined from the sideslip time history using the logarithmic decrement method. Depending on the resulting damping ratio, the ratio ϕ_{OSC}/ϕ_{AV} is then determined from the first two or three bank angle peaks according to equation (39).

The limit on sideslip excursions uses the ratio of the maximum change in sideslip to the initial peak magnitude in roll response, $|\Delta\beta/\phi_1|$, as criterion parameter. Here $|\Delta\beta|$ is the maximum change in sideslip within the time $t_{\Delta\beta} = \min(6 \text{ sec.}, T_d/2)$. In addition, if the ratio of the amplitudes of the bank angle and sideslip amplitudes, $|\phi/\beta|_d$, exceeds 0.2, the product $0.2 \times |\Delta\beta/\phi_1| \times |\phi/\beta|_d$ is to be used as an additional criterion parameter (see [47]).

In FitlabGui, $t_{\Delta\beta}$ is determined automatically. The sideslip change $\Delta\beta$ as well as $t_{1\beta}$ are determined by marking the minimum and maximum sideslip values. ψ_β can then be determined from equation (40).

For the last step, the free responses of bank angle and sideslip are approximated by the following analytical functions:

(41)
$$\phi_{model} = A_\phi e^{-\zeta_d\omega_d(t-t_0)}\cos\left(\omega_d\sqrt{1-\zeta_d^2}(t-t_\phi)\right) + e^{-B_\phi(t-t_0)} + \phi_{BIAS}$$

(42)
$$\beta_{model} = A_\beta e^{-\zeta_d\omega_d(t-t_0)}\cos\left(\omega_d\sqrt{1-\zeta_d^2}(t-t_\beta)\right) + \beta_{BIAS}$$

Once the model parameters (A_ϕ, t_ϕ, B_ϕ, ϕ_{BIAS} for the bank angle, A_β, t_β, β_{BIAS} for the sideslip) have been determined, ϕ/β is determined from the ratio of the envelopes of the two model equations.

Figure 12 shows an example for the measured roll and sideslip angles in blue and the corresponding model outputs in red. The envelopes of the models are shown in black.

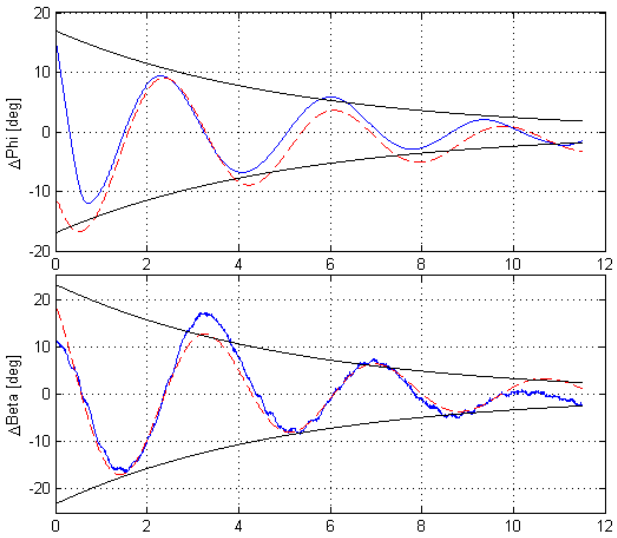

Figure 12: Approximation of roll and sideslip angles

6.2. Utilities

In addition to the parameters of the quantitative criteria described in the previous subsection, FitlabGui allows to calculate the following parameters:

- RMS / Cutoff Frequency
- Attack Parameter

6.2.1. RMS / Cutoff Frequency

Let δ be a control input signal with an autospectrum $G_{\delta\delta}$. The root mean square (RMS) value σ_1 of this control input for the frequency range $[O, \omega_1]$ is calculated by integrating the power spectrum over the specified frequency range

$$\sigma_1^2 = \frac{1}{2\pi} \int_0^{\omega_1} G_{\delta\delta} d\omega \tag{43}$$

Similarly, the total RMS σ_{tot} is determined from

$$\sigma_{tot}^2 = \frac{1}{2\pi} \int_0^{\infty} G_{\delta\delta} d\omega \tag{44}$$

The pilot cutoff frequency ω_{CO} is defined as the half-power frequency. That means, ω_{CO} is the frequency ω_1 such that

$$\left(\frac{\sigma_1}{\sigma_{tot}}\right)^2 = 0.5 \quad \text{or} \quad \frac{\sigma_1}{\sigma_{tot}} = \sqrt{0.5} = 0.707 \tag{45}$$

According to control theory, the pilot cutoff frequency as obtained above is a good estimate of the pilot/vehicle broken-loop gain crossover frequency.

6.2.2. Attack Parameter

The control attack parameter as introduced in [52] measures the size and rapidity of pilot control inputs. It is defined as

$$P_{attack} = \frac{\dot{\delta}_{pk}}{\Delta\delta} \tag{46}$$

where δ is the pilot control deflection. This means that P_{attack} is the ratio of the peak control input rate $\dot{\delta}_{pk}$ to the difference $\Delta\delta$ of the control inputs at the beginning and the end of the regarded time interval.

For the calculation of the attack parameter, the control input signal has first to be filtered to remove noise and to allow determining the control input rate $\dot{\delta}$ by numerical differentiation. Next, the control reversals, i.e. the time points where the input rate changes sign, have to be located. Each interval between two control reversals corresponds to one attack point and yields one value for P_{attack}. Intervals with control input changes $\Delta\delta$ below a certain lower threshold (usually 0.5%) are neglected.

In addition to the attack parameters, the following parameters are also of interest and are therefore determined in FitlabGui.

1. Attack number: The total number of times that the pilot moves the control by more than the lower threshold.
2. Attack number per second: The attack number expressed in terms of the average number of control movements per second.
3. Mean attack rate: The mean rate at which the pilot is moving his control.
4. Mean control displacement: The mean of the control displacements measured for each of the attack points.

6.3. MTE Plots

A more mission-oriented approach to helicopter handling qualities is taken by the Mission Task Elements (MTEs). The ADS-33 contains 23 MTEs that are supposed to cover the main tasks that occur during operation (e.g. hover, acceleration/deceleration, various turns, landing).

Each MTE has a definite start and finish as well as prescribed temporal and spatial preformance requirements. The limits for desired and adequate performance of each MTE depend on the rotorcraft category (attack, scout, utility, cargo) and the visual environment (good, degraded).

For performing mission task element maneuvers with the ACT/FHS helicopter both in the simulator and in flight tests, several MTE displays have been defined. Figure 13 shows the MTE display for the hover task as an example. The MTE displays are designed to help the pilot perform the specific maneuver and thus show the limits for desired and adequate performance.

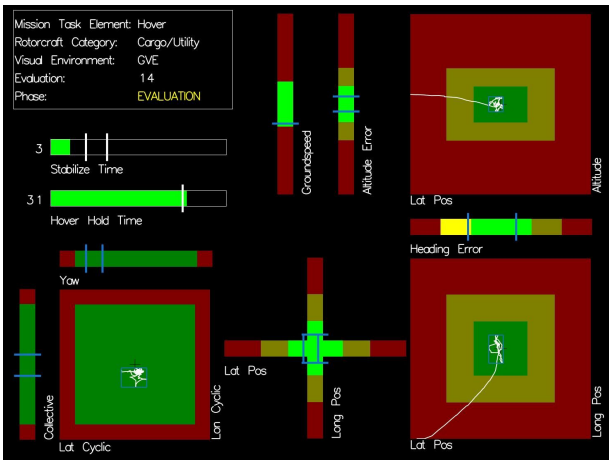

Figure 13: MTE Hover Display

Application examples for using these MTE displays include HQ investigations regarding active sidesticks [53, 54] and load placement tasks [55, 56].

All signals that are used in these MTE displays are recorded in the ACT/FHS datasets and thus are available for evaluating the MTE tests. So far, standardized plots from ACT/FHS data for the following mission task elements have been defined:

- Hover
- Vertical Maneuver
- Lateral Reposition
- Depart / Abort
- Hovering Turn
- Slalom
- Pirouette
- Load Placement

Figure 14 shows an example of a corresponding MTE evaluation plot for the hover maneuver. In the time history diagrams in the upper half, vertical lines mark the transition between the maneuver phases (start, deceleration, stabilization). Shown are the time histories for the time within each maneuver phase, ground speed, height and heading. The control activity is displayed in the lower left and the helicopter position in the lower right. Where applicable, yellow and red lines mark the limits for desired and adequate performance for the corresponding maneuver phases and thus allow to quickly assess the quality of the performed maneuver.

7. MISCELLANEOUS FEATURES

All plot windows produced by FitlabGui are normal MATLAB figures. Therefore, their appearance can be modified using the options of the figure menus or by issuing the corresponding commands from the MATLAB command window.

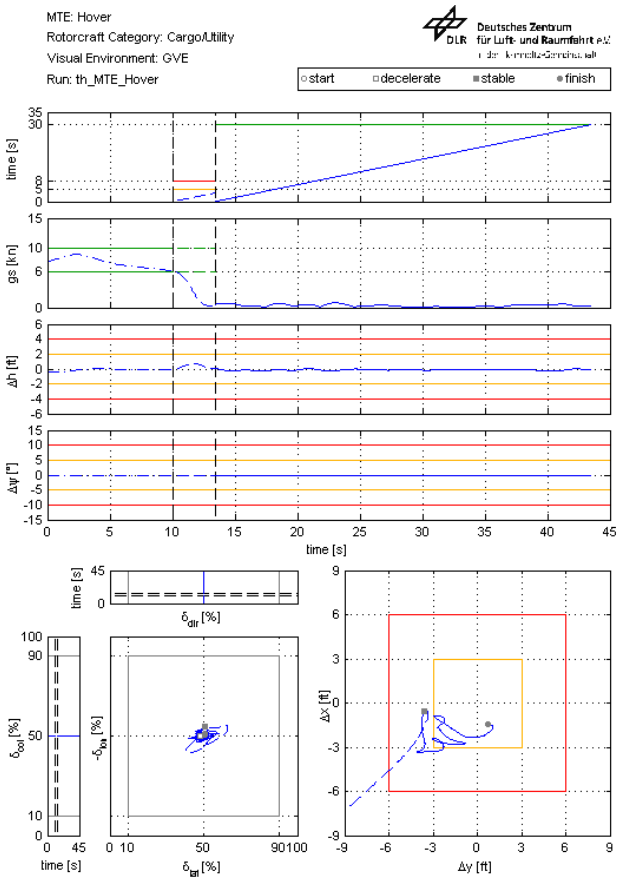

Figure 14: Example for MTE Hover Plot

All current settings of FitlabGui can be saved in so-called project files. This allows to easily

- apply unit conversions and calculations to new data
- recreate plots or apply them to new data
- save interim results during system identification

Logfiles can be created for system identification calculations and handling qualities evaluations.

For batch processing, the system identification part of FitlabGui can be run from the command line.

When linear or polynomial models are identified, the identified models are made available as LTI objects (state space (SS) for linear models and transfer function (TF) or zero-pole gain (ZPK) for polynomial models) and are thus readily available for further processing within MATLAB.

Each identification run can automatically be followed by a call to a user-defined post-processing routine that has access to all identification results (including the accuracy information). This allows for example to create special plots or to save identification results to a file or database.

8. SUMMARY

The MATLAB-based software tool FitlabGui, that was developed at the DLR Institute of Flight Systems, integrates routines for

- data preprocessing
- frequency response generation
- data visualization and analysis
- system identification, and
- helicopter HQ analysis

The software thus allows to perform most tasks necessary for time domain and frequency domain data analysis and model development within one tool.

The software package has been successfully used in projects with various types of vehicles, such as fixed-wing aircraft, miniature and full-scale helicopters, gyrocopters, and parafoils.

COPYRIGHT STATEMENT

REFERENCES

[1] Hamel, P. and Jategaonkar, R., "Evolution of Flight Vehicle System Identification," *Journal of Aircraft*, Vol. 33, No. 1, Jan-Feb 1996, pp. 9–28.

[2] Hamel, P. and Jategaonkar, R., "The Role of System Identification for Flight Vehicle Applications - Revisited," *RTO-MP-11*, Mar 1999, Paper 2.

[3] Plaetschke, E. and Mackie, D. B., "Maximum-Likelihood Schätzung von Parametern linearer Systeme aus Flugversuchsdaten - Ein FORTRAN-Programm," Mitt. 84-10, DFVLR, Jan 1984.

[4] Jategaonkar, R. and Plaetschke, E., "Maximum-Likelihood Estimation of Parameters in Linear Systems with Process and Measurement Noise," FB 87-20, DFVLR, Jun 1987.

[5] Marchand, M. and Fu, K. H., "Frequency Domain Parameter Estimation of Aeronautical Systems with and without Time Delay," *Proceedings of the 7th IFAC Symposium on Identification and System Parameter Estimation*, York, UK, Jul 1985.

[6] Jategaonkar, R. and Thielecke, F., "ESTIMA - An Integrated Software Tool for Nonlinear Parameter Estimation," *Aerospace Science and Technology*, Vol. 6, No. 8, 2002, pp. 565–578.

[7] Ismail, S., von Gruenhagen, W., Hamers, M., and Pausder, H.-J., "HAT - A Handling-qualities Analysis Toolbox for Rotorcraft and Aircraft," *29th European Rotorcraft Forum*, Friedrichshafen, Germany, Sep 2003.

[8] Seher-Weiss, S., "FitlabGui - A MATLAB Tool for Flight Data Analysis and Parameter Estimation - Version 2.5," IB 111-2015/34, DLR, Dec 2015.

[9] Seher-Weiss, S., "Heli-HQ: An Add-On to FITLAB for Helicopter Handling Qualities Analysis," IB 111-2015/01, DLR, Jan 2015.

[10] National Space Science Data Center NASA/Goddard Space Flight Center, Greenbelt, Maryland 20771, *CDF User's Guide Version 3.0*, 2005.

[11] Rabiner, L. and Gold, B., *Theory and Application of Digital Signal Processing*, Prentice Hall, Englewood Cliffs, New Jersey, 1975.

[12] Bendat, J. and Piersol, A., *Engineering Applications of Correlation and Spectral Analysis*, John Wiley & Sons, New York, 2nd ed., 1993.

[13] Press, W., Teukolsky, S., Vetterling, W., and Flannery, B., *Numerical Recipes in C*, Cambridge University Press, New York, 1992.

[14] Sridhar, J. and Wulff, G., "Application of Multiple-Input/Single-Output Analysis Procedures to Flight Test Data," *Journal of Guidance, Control, and Dynamics*, Vol. 14, No. 3, May-June 1991, pp. 645–651.

[15] Ockier, C. J., "The Art of Frequency Response Calculation," IB 111-97/07, DLR, Feb 1997.

[16] Bendat, J. and Piersol, A., *Random Data: Analysis and Measurement Procedures*, John Wiley & Sons, New York, 2nd ed., 1986.

[17] Tischler, M. B. and Remple, R. K., *Aircraft and Rotorcraft System Identification: Engineering Methods with Flight-Test Examples*, AIAA Education Series, American Institute of Aeronautics and Astronautics, Reston, VA, 2nd ed., 2012.

[18] Pintelon, R. and Schoukens, J., *System Identification: A Frequency Domain Approach*, John Wiley & Sons, Inc., 2nd ed., 2012.

[19] Fragniére, B. and Wartmann, J., "Local Polynomial Method Frequency-Response Calculation for Rotorcraft Applications," *AHS 71st Annual Forum*, Virginia Beach, Virginia, May 2015.

[20] Schoukens, J., Vandersteen, G., Rolain, Y., and Pintelon, R., "Frequency Response Function Measurements Using Concatenated Subrecords With Arbitrary Length," *IEEE Transactions on Instrumentation and Measurement*, Vol. 61, No. 10, Oct 2012, pp. 2682–2688.

[21] N.N., “Flying Qualities of Piloted Aircraft,” USAF MIL-STD-1797B, Dept. of Defense Handbook, Dec 1997.

[22] Jategaonkar, R., *Flight Vehicle System Identification: A Time Domain Methodology*, Vol. 245 of *Progress in Astronautics and Aeronautics*, American Institute of Aeronautics and Astronautics, Reston, VA, 2nd ed., 2015.

[23] Jategaonkar, R., Behr, R., Gockel, W., and Zorn, C., “Data Analysis of Phoenix Reusable Launch Vehicle Demonstrator Flight Test,” *Journal of Aircraft*, Vol. 43, No. 6, Dec 2006, pp. 1732–1737.

[24] Jann, T. and Greiner-Perth, C., “Flight Test Instrumentation for Evaluation of the FASTWing CL System,” *20th AIAA Aerodynamic Decelerator Systems Technology Conference and Seminar*, Seattle, Washington, May 2009, AIAA 2009-2932.

[25] Yakimenko, O. and Jann, T., *Precision Aerial Delivery Systems: Modeling, Dynamics and Control*, Vol. 248 of *Progress in Astronautics and Aeronautics*, chap. Parametrical Identification of Parachute Systems, American Institute of Aeronautics and Astronautics, Reston, VA, 2015, pp. 353–390.

[26] Dittmer, A. and Seher-Weiss, S., “Dynamic Calibration of the Noseboom Sensors of the Flying Helicopter Simulator,” *Deutscher Luft- und Raumfahrtkongress*, Hamburg, Germany, Sep 2010.

[27] Pruter, I. and Duda, H., “A New Flight Training Device for Modern Lightweight Gyroplanes,” *AIAA Modeling and Simulation Technologies Conference*, Portland, Oregon, Aug 2011, AIAA 2011-6497.

[28] Duda, H. and Pruter, I., “Flight Performance of Lightweight Gyroplanes,” *28th International Congress of the Aeronautical Sciences*, Brisbane, Australia, Sep 2012.

[29] de Oliveira Silva, B. G. and Mönnich, W., “System Identification of Flexible Aircraft in Time Domain,” *AIAA Atmospheric Flight Mechanics Conference*, Minneapolis, Minnesota, Aug 2012, AIAA 2012-4412.

[30] Schwithal, J., Rohlf, D., Looye, G., and Liersch, C., “An Innovative Route from Wind Tunnel Experiments to Flight Dynamics Analysis for a Highly Swept Flying Wing,” *Deutscher Luft- und Raumfahrtkongress*, Rostock, Germany, Sep 2015.

[31] Fezans, N., Schwithal, J., and Fischenberg, D., “In-Flight Remote Sensing and Characterization of Gusts, Turbulence, and Wake Vortices,” *Deutscher Luft- und Raumfahrtkongress*, Rostock, Germany, Sep 2015.

[32] Deiler, C., “Time Domain Output Error System Identification of Iced Aircraft Aerodynamics,” *Deutscher Luft- und Raumfahrtkongress*, Rostock, Germany, Sep 2015.

[33] Lorenz, S. and Chowdhary, G., “Non-Linear Model Identification for a Miniature Rotorcraft - Preliminary Results,” *American Helicopter Society 61th Annual Forum*, Grapevine, Texas, Jun 2005.

[34] Seher-Weiss, S. and von Gruenhagen, W., “EC 135 System Identification for Model Following Control and Turbulence Modeling,” *1st CEAS European Air and Space Conference 2007*, Berlin, Germany, Sep 2007, CEAS-2007-275.

[35] Seher-Weiss, S. and von Grünhagen, W., “Comparing Explicit and Implicit Modeling of Rotor Flapping Dynamics for the EC 135,” *CEAS Aeronautical Journal*, Vol. 5, No. 3, Sep 2014, pp. 319–332. doi:10.1007/s13272-014-0109-0.

[36] Seher-Weiss, S., “Comparing Different Approaches for Mmodeling the Vertical Motion of the EC 135,” *CEAS Aeronautical Journal*, Vol. 6, No. 3, Sep 2015, pp. 395–406. doi:10.1007/s13272-015-0150-7.

[37] Greiser, S., “Uncertainties in Modeling Helicopter Dynamics: A Framework Applied to System Identification Results,” *European Rotorcraft Forum*, Munich, Germany, Sep 2015.

[38] Brieger, O., Ossmann, D., Rüdinger, M., and Heller, M., “A New Flight Test Technique for Pilot Model Identification,” *AIAA Atmospheric Flight Mechanics Conference and Exhibit*, Honolulu, Hawaii, Aug 2008, AIAA 2008-6556.

[39] Niewind, I., “A New Approach for the Validation of Potential Pilot Gain Measures,” *EuroGNC 2013, 2nd CEAS Specialist Conference on Guidance, Navigation & Control*, Delft, The Netherlands, Apr 2013.

[40] Lusardi, J. A., von Gruenhagen, W., and Seher-Weiss, S., “Parametric Turbulence Modeling for Rotorcraft Applications - Approach, Flight Tests and Verification,” *Rotorcraft Handling Qualities Conference*, AHS, Liverpool, UK, Nov 2008.

[41] Nonnenmacher, D. and Müllhäuser, M., “Optimization of the Equivalent Mechanical Characteristics of Active Side Sticks for Piloting a Controlled Helicopter,” *60. Deutscher Luft- und Raumfahrtkongress*, Bremen, Germany, Sep 2011.

[42] Jategaonkar, R., “Bounded-Variable Gauss-Newton Algorithm for Aircraft Parameter Estimation,” *Journal of Aircraft*, Vol. 37, No. 10, 2000, pp. 742–744.

[43] Nelder, J. and Mead, R., “A Simplex Method for Function Minimization,” *The Computer Journal*, Vol. 7, 1965, pp. 308–313.

[44] Rowan, T., *Functional Stability Analysis of Numerical Algorithms*, PhD Thesis, University of Texas at Austin, 1990.

[45] Beck, R., “Parameteridentifizierung bei Systemen mit Unstetigkeiten,” IB 111-2004/06, DLR, Jan 2004.

[46] Subrahmanyam, M. B., “An Extension of the Simplex Method to Constrained Optimization,” *Journal of Optimization Theory and Applications*, Vol. 62, No. 2, 1989, pp. 311–319.

[47] N.N., “Handling Qualities Requirements for Military

Rotorcraft," ADS-33E-PRF: Aeronautical Design Standard, Performance Specification, United States Army Aviation and Missile Command, Aviation Engineering Directorate, Mar 2000.

[48] Höfinger, M., Blanken, C. L., and Strecker, G., "Evaluation of Aeronautical Design Standard 33E Cargo Helicopter Requirements - Flight Tests with a CH-53G," *32nd European Rotorcraft Forum*, Maastricht, Netherlands, 2006.

[49] Höfinger, M. and Blanken, C. L., "Flight Testing the ADS-33E Cargo Helicopter Handling Qualities Requirements Using a CH-53G," *Journal of the American Helicopter Society*, Vol. 58, No. 1, Jan 2013, pp. 1–11.

[50] Hoh, R. H., Mitchell, D. G., Blanken, C. L., and Key, D. L., "Test Guide for ADS-33E-PRF," HAI Technical Report 1130-1, Hoh Aeronautics, Inc., Apr 2008.

[51] Ockier, C., "Evaluation of the ADS-33D Handling Qualities Criteria Using the BO 105 Helicopter," FB 98-07, DLR, Jan 1998.

[52] Perfect, P., White, M. D., Padfield, G. D., and Gubbels, A. W., "Rotorcraft Simulation Fidelity - New Methods for Quantification and Assessment," *The Aeronautical Journal*, Vol. 117, No. 1188, Mar 2013.

[53] von Grünhagen, W., Schönenberg, T., Lantzsch, R., Lusardi, J. A., Lee, D., and Fischer, H., "Handling Qualities Studies into the Interaction Between Active Sidestick Parameters and Helicopter Response Types," *CEAS Aeronautical Journal*, Vol. 5, No. 1, 2014, pp. 13–28. doi:10.1007/s13272-013-0079-7.

[54] von Grünhagen, W., Müllhäuser, M., Höfinger, M., and Lusardi, J. A., "In-Flight Evaluation of Active Sidestick Parameters with Respect to Handling Qualities for Rate Command and Attitude Command Response Types," *Rotorcraft Handling Qualities Specialists' Meeting*, AHS, Huntsville, AL, Feb 2014.

[55] Nonnenmacher, D. and Jones, M., "Handling Qualities Evaluation of an Automatic Slung Load Stabilization System for the ACT/FHS," *41st European Rotorcraft Forum*, Munich, Germany, Sep 2015.

[56] Kim, H.-M., Nonnenmacher, D., Götz, J., Weber, P., von Hinüber, E., and Knedlik, S., "Initial Flight Tests of an Automatic Slung Load Control System for the ACT/FHS," *CEAS Aeronautical Journal*, Vol. 7, No. 2, Jun 2016, pp. 209–224. doi:10.1007/s13272-016-0181-8.